doi:10.1006/mthe.2002.0812

In Vivo Correction of Murine Tyrosinemia Type I by DNA-Mediated Transposition

Eugenio Montini,[1] Patrice K. Held,[1] Meenakshi Noll,[1] Nicolas Morcinek,[1] Muhsen Al-Dhalimy,[1] Milton Finegold,[2] Stephen R. Yant,[3] Mark A. Kay,[3] and Markus Grompe[1,*]

[1]*Department of Medical & Molecular Genetics and* [4]*Department of Pediatrics, Oregon Health and Sciences University, Portland, Oregon 97239*
[2]*Department of Pathology, Texas Children's Hospital, Baylor College of Medicine, Houston, Texas 77030*
[3]*Department of Pediatrics, Stanford University School of Medicine, Stanford, California 94305*

**To whom correspondence and reprint requests should be addressed at the Department of Molecular and Medical Genetics L103, 3181 SW Sam Jackson Park Road, Portland, OR 97201. Fax: (503) 494-6886. E-mail: grompem@ohsu.edu.*

Gene therapy applications of naked DNA constructs for genetic disorders have been limited because of lack of permanent transgene expression. This limitation, however, can be overcome by the *Sleeping Beauty* (SB) transposable element, which can achieve permanent transgene expression through genomic integration from plasmid DNA. To date, only one example of an *in vivo* gene therapy application of this system has been reported. In this report, we have further defined the activity of the SB transposon *in vivo* by analyzing the expression and integration of a fumarylacetoacetate hydrolase (FAH) transposon in FAH-deficient mice. In this model, stably corrected FAH^+ hepatocytes are clonally selected and stable integration events can therefore be quantified and characterized at the molecular level. Herein, we demonstrate that SB-transposon-transfected hepatocytes can support significant repopulation of the liver, resulting in long-lasting correction of the FAH-deficiency phenotype. A single, combined injection of an FAH-expressing transposon plasmid and a transposase expression construct resulted in stable FAH expression in ~1% of transfected hepatocytes. The average transposon copy number was determined to be ~1/diploid genome and expression was not silenced during serial transplantation. Molecular analysis indicated that high-efficiency DNA-mediated transposition into the mouse genome was strictly dependent on the expression of wild-type transposase.

INTRODUCTION

Transposon technology has been widely used as a molecular genetic tool in plants, bacteria, fungi, and insects [1]. For the experimental manipulation of vertebrate genomes, transposons from the Tc1/*mariner* superfamily have been used. Among these, the *Sleeping Beauty* (SB) element, a reconstructed version of the Tc1/*mariner*-like transposon from fish, is of particular interest [2] because it is able to transpose at a frequency superior to other elements of the same family [3]. The SB element transposes by a cut-and-paste mechanism that requires the binding of an element-encoded enzyme, the SB transposase, to short inverted-repeat (IR) sequences flanking the transposon [4]. These elements do not require host-specific factors for their activity *in vitro* [5,6] and actively transpose from plasmid or genomic DNA into the chromosomal DNA of a wide variety of species such as bacteria [7], mosquito [8] zebrafish [9,10], and chicken [11] and human cells [2,12,13] and mouse embryonic stem cells [14]. The SB element has been used in experimental manipulation of the mammalian genome mainly for germ-line transgenesis [15] and gene targeting [3,16]. However, the SB transposon also holds promise for gene therapy applications, because it combines the capacity of stable integration with the use of simple plasmid DNA. In contrast to viral gene therapy vectors, naked DNA is easy and affordable to produce in large scales and much less immunogenic. Recent advances have made it possible to transfect several cell types efficiently with naked DNA *in vivo,* especially muscle and liver [17]. Nonetheless, there is currently only one published report of an *in vivo* gene therapy application of SB transposase [18]. Hemophilic mice deficient in factor IX ($FIX^{-/-}$) were injected with a two-plasmid SB system. One plasmid contained an expression cassette for the FIX cDNA surrounded by the SB-IR sequences and the second plasmid expressed the SB transposase. Mutant mice treated with these constructs had significantly improved clotting function, and transposase-dependent stable integration was demonstrated [18]. Because of the promise of the SB transposon revealed

1525-0016/02 $35.00

doi:10.1006/mthe.2002.0812

by these experiments, further characterization and testing *in vivo* were justified.

We chose to study DNA transposition in a mouse model of hereditary tyrosinemia type 1 (HT1) [19], because of its unique advantages for the characterization of stable integration events in hepatocytes *in vivo*. HT1 is a lethal recessive liver disease caused by deficiency of fumarylacetoacetate hydrolase (FAH) [19], the enzyme that catalyzes the last step in tyrosine degradation. In the HT1 liver, FAH-expressing hepatocytes display a strong proliferative advantage, grow clonally to form nodules, and repopulate the entire diseased liver mass [20,21]. Because of this selective advantage, phenotypic recovery can be achieved by any technique that results in stable FAH expression, including cell transplantation therapy [22,23] or virus-mediated gene transfer [20,22,24–26].

In this report, we took advantage of the characteristics of this model to study the SB transposon system further *in vivo*. We show that *Sleeping Beauty* can permanently transfect hepatocytes, resulting in phenotypic correction of murine HT1. The frequency of and nature of the integration events in mouse liver tissue were also determined.

RESULTS

We used the unique biology of the FAH knockout mouse to answer several questions regarding the behavior of the *Sleeping Beauty* gene transfer system in the liver *in vivo*. First, we wanted to know the rate of stable integration and gene expression. Second, we wished to determine whether gene expression was stable and could result in phenotypic rescue of the liver disease. Finally, the nature (copy number, sequences of integration sites) of the integration events was of interest.

Frequency of Stable Integration

Histochemical markers such as *Escherichia coli* lacZ or alkaline phosphatase can be utilized to determine the frequency of stable gene expression in liver [37,38]. However, this method does not necessarily permit the determination of the frequency of vector integration, because stable gene expression can also be observed in the absence of integration [39]. Adeno-associated virus (AAV) vectors and even simple plasmid constructs can produce such long-term expression [25,26]. In the FAH knockout liver, however, single FAH^+ hepatocytes can selectively expand and form clonal nodules only if stable integration has occurred resulting in FAH expression in the daughters of the initially transfected hepatocytes [20,25]. This characteristic can be exploited to determine rigorously the frequency with which a given gene transfer system results in both integration and stable gene expression. We injected FAH mutant mice hydrodynamically with transposon DNA while they were on 2-(2-nitro-4-trifluoromethylbenzoyl)-1,3-cyclohexanedione (NTBC). To measure the initial transfection frequency of hepatocytes, some animals were harvested and liver sections were stained for FAH expression on day 3 after injection. Microscopic examination showed that only ~0.5% of hepatocytes were FAH^+ at this time-point (Table 1). Few animals had higher levels (10%) consistent with previously reported results obtained with hydrodynamic injection [40]. The reason for this lower than expected initial transfection frequency is unclear, but may be related to the strain of mouse used here, since control injections in wild-type mice using lacZ-based reporters yielded frequencies of 5–12% (data not shown). Alternatively, FAH expression may still be relatively low on day 3 after injection, resulting in an underestimation of the true transfection frequency.

TABLE 1: Initial transduction efficiency

Group 1	Group 2	Group 3	Group 4
WT-SB + pT-FAH	mut-SB + pT-FAH	SBcis	pT-FAH alone
0.7 ± 1.1	0.3 ± 1.1	0.5 ± 0.2	1.2 ± 2.1
3	5	11	5

The average percentage ± standard deviation of FAH^+ cells on day 3 after hydrodynamic injection is given for different plasmid combinations used. The bottom row indicates the number of FAH mutant mice analyzed.

For measurement of the integration frequency, we injected four groups of $FAH^{-/-}$ mice with the following experimental plasmids and controls: group 1 ($n = 7$), FAH transposon (pT-hFAH) plus the expression construct for wild-type transposase (pCMV-SB); group 2 ($n = 2$), pT-hFAH plus the expression construct for mutant SB transposase (pCMV-mSB); group 3 ($n = 9$), construct containing the FAH transposon and SB transposase *in cis* (pT-hFAH-SBcis); group 4 ($n = 4$), pT-hFAH only. In groups 1 and 2, the previously determined [18] optimal ratio of 1 μg of the transposase expression construct (pCMV-SB or pCMV-mSB) and 25 μg of the transposable element pT-hFAH was used. On day 7 after plasmid injection NTBC was discontinued to permit the development of liver disease and formation of hepatocyte nodules. All animals were harvested on day 25 following injection. The frequencies of FAH^+ nodules and FAH^+ single hepatocytes were quantitatively determined and the results are summarized in Fig. 1 and Table 2.

In liver sections from group 1 (mice treated with wild-type transposase *in trans*), the average absolute frequency of FAH^+ nodules was $7.3 \pm 9.8 \times 10^{-5}$ (1/13,700). The nodule frequency ranged from a maximum of 1/3600 in the best mouse to 1/165,000 in the worst.

The absolute frequency of FAH^+ nodules only as a measurement of stable integration is the most conservative and is probably an underestimation. However, it is likely that several single FAH^+ hepatocytes on day 25 are also products of chromosomal integration. This view is supported by the high frequency of single FAH^+ hepatocytes in the group treated with the wild-type transposase and the absence of any single cells in groups 3 and 4 that

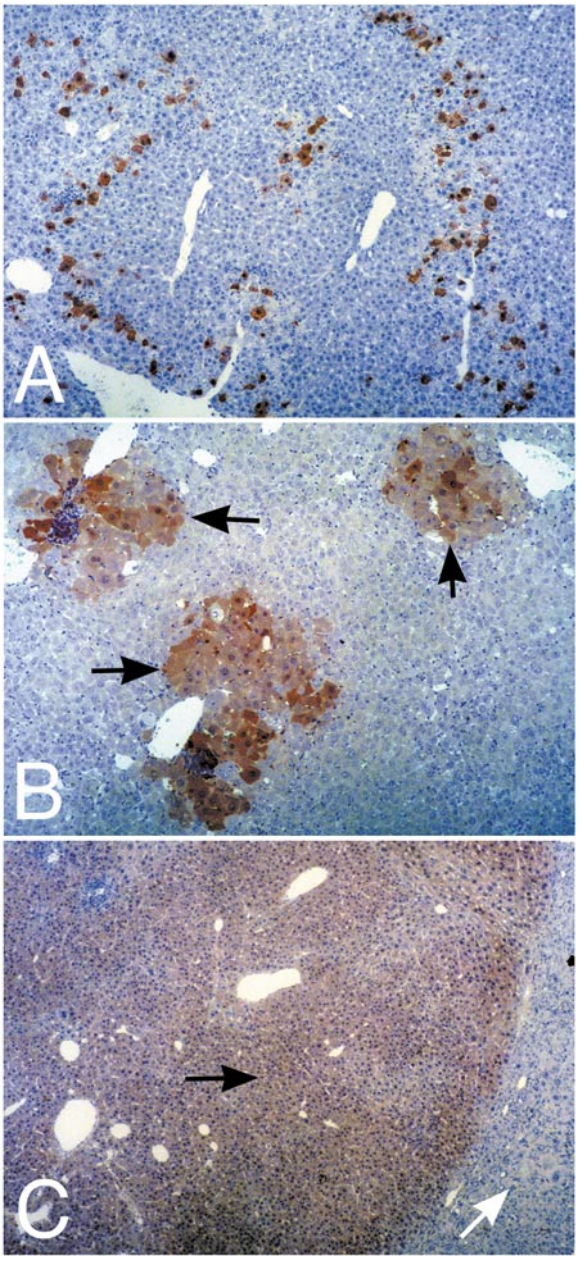

FIG. 1. FAH immunohistochemistry. Examples of FAH immunohistochemistry in mice treated with pT-hFAH and wild-type SB transposase during the repopulation process. Brown straining shows FAH^+ hepatocytes. (A) Day 2 after injection. Original magnification 100×. A field with ~5% FAH-positive single cells is shown. (B) Day 25 after injection. Original magnification 400×. Three large nodules of FAH-positive hepatocytes (black arrows) are shown. (C) Day 90 after injection. Original magnification 50×. Large, confluent areas of FAH-positive cells (black arrow) lie adjacent to residual pockets of FAH-deficient cells (white arrow).

did not receive any wild-type transposase. If single FAH^+ hepatocytes were also counted as integration events, the absolute integration frequency in group 1 increased to an average of $2.6 \pm 3.1 \times 10^{-4}$ (1/3815). The highest absolute frequency observed in a single animal was 1/1100.

In all other groups (2, 3, and 4), the relative frequency of either the nodules or the single FAH^+ hepatocytes was at least 10 times lower. No FAH-positive cells or clusters were observed in animals injected with the FAH transposon alone (group 4) and no transposase. Clearly, the *cis* construct (group 3), in which both transposon and transposase resided in the same plasmid, did not result in efficient transposition.

We also calculated the integration efficiency estimates considering the initial transfection efficiency after hydrodynamic injection and after correction for the sampling effects caused by the nodule size. The precise initial transfection frequencies for the animals harvested on day 25 after injection cannot be measured, but have been estimated based on control animals harvested 3 days after injection. We performed calculations for both the observed average transfection frequency of 0.5% obtained with FAH expression constructs (see Table 1) and the maximal observed transfection efficiency of 10%. These results are summarized in Table 3.

In group 1, injected with the FAH transposon and wild-type SB transposase, the best estimate (using the actual observed initial transfection frequency) of the corrected integration frequency was an average of 4% (1/25). This number is very close to the estimates of Yant *et al.* [18]. As expected, the frequency of integration in each of the control groups was much lower.

Phenotypic Rescue

The formation of FAH^+ nodules described above clearly indicated that SB resulted in stable integration and expression of the transgene. We wished also to determine whether transposon-based gene expression was sufficiently high enough to cure the tyrosinemia, whether it was stable long-term, and whether any adverse events (for example, tumor formation) were detectable in transposon-transfected cells. Therefore, to analyze the therapeutic potential of the FAH-SB transposon system, we injected a total of 26 $FAH^{-/-}$ mice with pT-hFAH in combination with either pCMV-SB ($n = 13$) or pCMV-mSB ($n = 13$). On day 7 after injection, animals were taken off NTBC to start the selection process. Between days 14 and 30, mice of both groups lost almost 30% of their initial body weight and some died from liver failure (Fig. 2A). To reduce the observed mortality NTBC treatment was subsequently reestablished at day 30 for 2 weeks (Fig. 2B). At the end of this recovery period, the mice were again taken off-NTBC (Fig. 2B). Sixty-two percent (8/13) of the mice treated with pT-hFAH and pCMV-SB survived up to 90 days off NTBC (the length of the study). These survival kinetics are consistent with the relatively low absolute integration frequency of <1/1000 shown in Ta-

doi:10.1006/mthe.2002.0812

TABLE 2: Absolute frequencies of FAH-positive hepatocytes

Plasmid combination	WT transposase ($n = 7$)	Mutant transposase ($n = 2$)	SBcis ($n = 9$)	pT-FAH only ($n = 4$)
Experimental group	1	2	3	4
Nodule frequency	$7.3 \pm 9.8 \times 10^{-5}$	$7.78 \pm 2.3 \times 10^{-6}$	$1 \pm 1.1 \times 10^{-5}$	
	1/13,700	1/128,000	1/101,000	0
Min	1/165,000	1/163,000	0	0
Median	1/46,500	1/128,000	1/156,000	0
Max	1/3600	1/106,000	1/37,200	0
Single HC frequency	$1.9 \pm 2.2 \times 10^{-4}$		$1 \pm 1.1 \times 10^{-5}$	
	(1/5300)	0	(1/98,000)	0
Min	0	0	0	0
Median	1/8700	0	1/104,000	0
Max	1/1500	0	1/28,500	0
Nodule + Single HC frequency	$2.6 \pm 3.1 \times 10^{-4}$	$7.8 \pm 2.3 \times 10^{-6}$	$2 \pm 2.1 \times 10^{-5}$	
	1/3815	1/128,000	1/50,000	0
Min	1/165,000	1/163,000	0	0
Median	1/6500	1/128,000	1/62,400	0
Max	1/1100	1/106,000	1/18,000	0

Absolute integration frequencies for the different plasmids. The calculations were made counting either FAH^+ nodules alone or both nodules and single cells as integration events. Averages with standard deviation are given. In addition, the minimum (Min, worst animal), median, and maximal (Max, best animal) frequencies in each group are shown. Two-tailed *t* tests showed statistically significant differences between the means in groups 1 and 3. Differences between 1 and 2 were not significant because of the low *n* in group 2.

TABLE 3: Corrected integration frequencies

Plasmid combination	WT transposase ($n = 7$)		Mutant transposase ($n = 2$)		SBcis ($n = 9$)		pT-FAH ($n = 4$)
Experimental group	1		2		3		4
Transduction efficiency	0.5%	10%	0.5%	10%	0.5%	10%	NA
Nodules	$4.5 \pm 5.6 \times 10^{-4}$	$2.2 \pm 2.9 \times 10^{-4}$	$4.4 \pm 1.2 \times 10^{-4}$	$2.2 \pm 2.9 \times 10^{-4}$	$6 \pm 6.4 \times 10^{-4}$	$2.9 \pm 3.2 \times 10^{-5}$	0
	1/230	1/4550	1/2140	1/4550	1/1680	1/33,500	
Min	1/2800	1/55,000	1/2700	1/55,000	0	0	
Median	1/780	1/15,500	1/2100	1/15,500	1/2600	1/52,000	0
Max	1/60	1/1200	1/1770	1/1200	1/620	1/12,400	
Nodules + single cells	$4 \pm 4.8 \times 10^{-2}$	$2.1 \pm 2.4 \times 10^{-3}$	$4.4 \pm 1.2 \times 10^{-4}$	$2.1 \pm 2.4 \times 10^{-3}$	$2.6 \pm 2.8 \times 10^{-3}$	$1.32 \pm 1.39 \times 10^{-4}$	0
	1/25	1/470	1/2140	1/470	1/380	1/7600	
Min	1/2800	1/55,000	1/2700	1/55,000	0	1/8700	
Median	1/40	1/825	1/2100	1/825	1/430	1/2400	0
Max	1/8	1/135	1/1800	1/35,000	1/120	1/2700	

The integration frequencies are given for the different plasmids. The calculations were made assuming initial transfection efficiencies of either 0.5 or 10% and counting either FAH^+ nodules alone or both nodules and single cells as integration events. Averages with standard deviation are given. In addition, the minimum (Min, worst animal), median, and maximal (Max, best animal) frequencies in each group are shown.

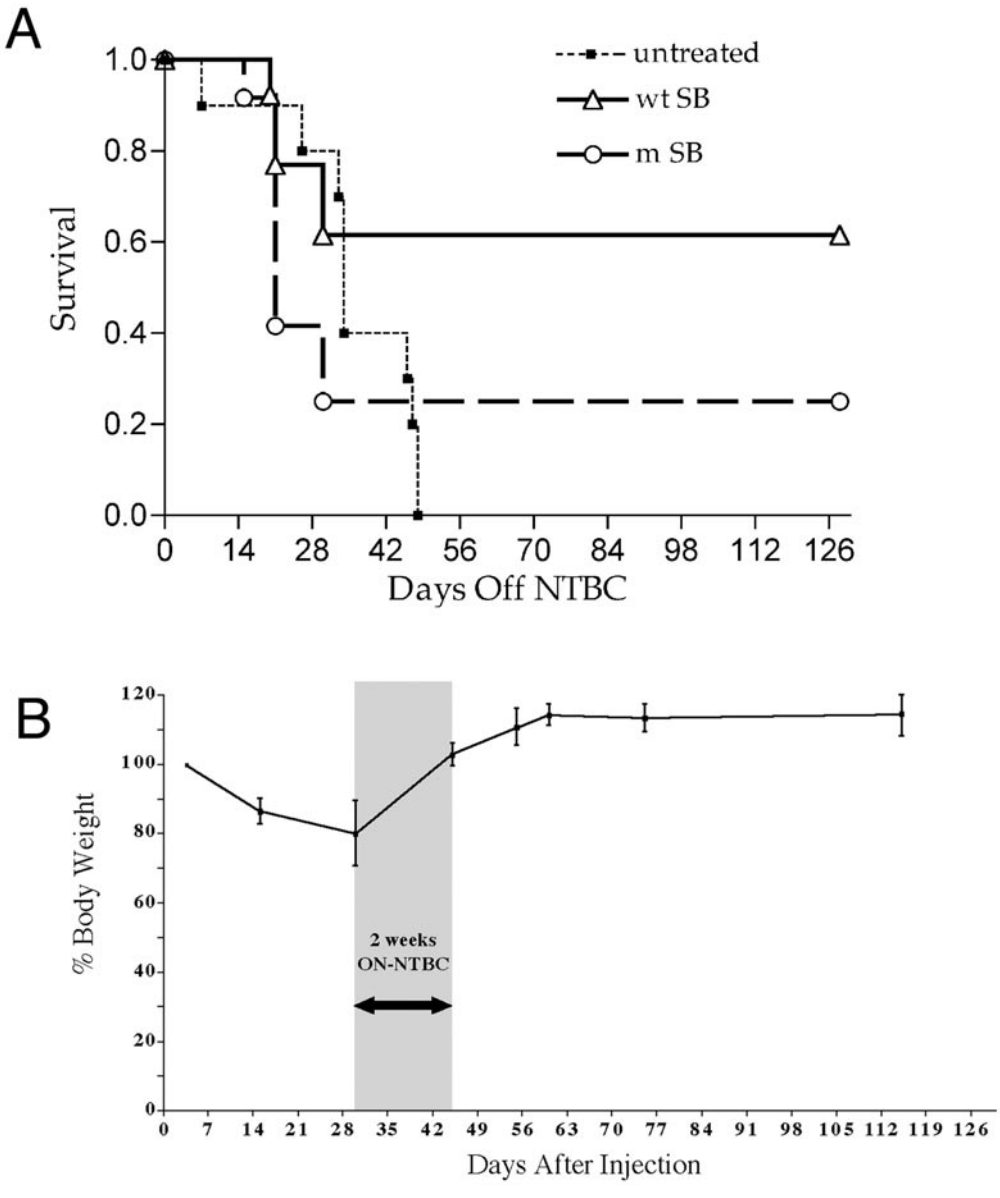

FIG. 2. Survival curves and weight gain of treated mice. (A) A total of 26 $FAH^{-/-}$ mice were injected with pT-hFAH in combination with either wild-type transposase (wt) or mutant transposase (m). Survival was better in the animals injected with wild-type transposase. In both groups, some animals survived for more than 4 months off NTBC (the end of the experiment). In contrast, untreated controls died by 7 weeks after NTBS withdrawal. (B) Body weight variation in surviving mice. On day 3 after injection the animals were taken off NTBC. At day 30, weight loss ranged between 10 and 30%. To reduce the mortality, mice were then treated with NTBC for 2 weeks. During this period all survivors gained the original body weight. At day 45 after injection the animals were again taken off NTBC. During this second period of selection all mice gained up to 120% of the original body weight and appeared healthy.

ble 2. Interestingly, 3/13 (23%) mice treated with pT-hFAH and pCMV-mSB also survived (Fig. 2A). This finding agrees with our previously reported results that absolute correction frequencies of as low as 1/500,000 can result in phenotypic rescue of FAH mutant mice [22,33]. All long-term survivors appeared healthy and gained up to 120% of their original body-weight (Fig. 2B). Hepatic functions were in the normal range (Table 4). Liver sections were immunostained to detect FAH^+ cells and revealed large areas of healthy FAH^+ hepatocytes (see Fig. 1C). These findings demonstrated that the frequency of stable transposon integration following a single injection of the wild-type SB transposon system was high enough to rescue the lethal $FAH^{-/-}$ phenotype (untreated mice die between 20 and 45 days after NTBC deprivation). However, stable integration and gene expression were observed even in the absence of wild-type transposase activity in a small number of mice.

To understand the differences between the groups treated with pT-hFAH and active or mutant transposase better, we performed a quantitative time course. Liver samples from mice from the two different groups (groups 1 and 2) were harvested at days 3 and 90 after stopping NTBC (n = 3 mice/time point). FAH^+ hepatocytes were identified by immunohistology. On day 3 after injection both experimental groups had the same number of FAH^+

doi:10.1006/mthe.2002.0812

TABLE 4: Liver and renal function tests

	Wild-type SB off NTBC	Serial transplant off NTBC	Mutant SB off NTBC	Wild-type SB on NTBC	Untreated off NTBC	Wild-type controls
ALT (U/L)	37 ± 41 (6)	52 ± 12 (3)	157 ± 102 (5)	20 ± 4 (4)	969 ± 583 (4)	70 ± 8 (7)
BC (mg/dl)	0.15 ± 0.2 (6)	0.09 ± 0.1 (3)	0.34 ± 0.27 (5)	0 (4)	4.5 (4)	0 (7)
BU (mg/dl)	0 (6)	0 (3)	0 (5)	0 (4)	0.5 (6)	0 (7)
CREAT (mg/L)	0.13 ± 0.07 (6)	ND	0.20 (5)	0.18 ± 0.05 (4)	1.5 ± 0.2 (9)	0.2 ± 0.1 (7)

Serum levels of alanine aminotransferase (ALT), conjugated bilirubin (BC), unconjugated bilirubin (BU), and creatinine (CREAT) were measured in mice treated with different experimental protocols. Animals were analyzed while either on NTBC or off NTBC for 6 weeks. Mice treated with wild-type transposase were analyzed during the first round of repopulation or after serial transplantation (tertiary recipients). ND, not determined.

hepatocytes (0.5%, see Table 1) and no FAH^+ nodules were identified. However, the level of repopulation was markedly different on day 90. Higher levels of repopulation (60 ± 12% vs 9 ± 7%) were observed when the construct expressing wild-type transposase was used. The higher death rate in mice injected with the mutant transposase construct also suggested that the low level of gene transfer achieved was insufficient for survival in most animals.

We documented the stability of the gene transfer further by performing serial transplantation experiments. Long-term survivors (>90 days) treated with pT-hFAH + pCMV-SB were used as hepatocyte donors for two serial transplantation experiments ($n = 4$) into naive $FAH^{-/-}$ recipient mice (three each per donor). All serially transplanted FAH mutant mice survived NTBC withdrawal and displayed normal health (no weight loss). Secondary recipients that had survived >90 days off NTBC were then used as donors for a second round of transplantation (transplanted with 10,000 or 500,000 hepatocytes) and again, all $FAH^{-/-}$ tertiary recipients were fully rescued (see Table 4). Importantly, no liver tumors were observed in any of the serial transplant recipients and the histology of the repopulating cells was normal (data not shown). The expansion of the initially transfected hepatocytes (1/1000 cells) to ~60% of the liver mass (3×10^7 cells) and two rounds of serial transplantation would require at least 30 rounds of cell doubling. Therefore, transposon-mediated FAH expression was remarkably stable and not associated with an increased incidence of transformation.

Integration Site Analysis

We also determined the nature of the transposon integration sites. Southern blot analysis of DNA from highly repopulated livers (>60% by immunohistochemistry) derived from long-term survivors (5 months off NTBC) was used to determine the copy number of integrated transposons and to ascertain whether the integration had occurred by transposition or by random integration. In the pT-hFAH plasmid *Pst*I restriction sites are located immediately adjacent to the inverted terminal repeat of the transposable element (see Fig. 3). This site is therefore expected to be lost during proper transposase-mediated integration, but preserved during most random insertion events. A second digestion with *Sac*I was used to distinguish between episomal and randomly integrated transposons. In addition, a constant transposon-specific and integration-independent band was compared to an internal, mouse genomic locus to measure the transposon copy number. Maps of the Southern blot strategy are given in Fig. 3A and the results are shown in Table 5 and Figs. 3B and 3C. In mice injected with pT-hFAH and the wild-type transposase, virtually all integration sites (>98%) had lost the flanking *Pst*I site, which indicates transposase-mediated integration. This was confirmed by the rescue of several integration sites via inverse PCR. The majority of integration sites (6/7) displayed the canonical TA dinucleotide at the expected location for SB-mediated integration (Table 6). Results of BLASTn analyses of the genomic portion suggest that the integration occurred at random locations in the genome. Importantly, the average copy number of FAH-positive cells was ~1/genome equivalent. The average corrected copy number (Table 5) was 0.78, consistent with the degree of repopulation observed by immunohistochemistry (>60%, but <100%). Therefore, each gene-transfected cell likely underwent only a single transposition event. Moreover, the lack of multiple integration sites and the low copy number indicate that most transposition events resulted in long-term FAH expression *in vivo*.

In contrast to the animals treated with wild-type SB, ~50% of the integration events (0.19/0.38, Table 5) in the mutant SB group resulted in retention of the *Pst*I site, consistent with random integration. Although ~50% of the integration events did not result in loss of the *Pst*I site, it is important to note that this does not necessarily signify integration by proper transposition. A breakpoint for random integration anywhere between the end of the FAH coding region and the *Pst*I site would also result in loss of the 1.6-kb fragment. The mutant transposase used has no transposition activity *in vitro* [18], making it very unlikely that the loss of the 1.6-kb fragment is due to transposase-mediated integration.

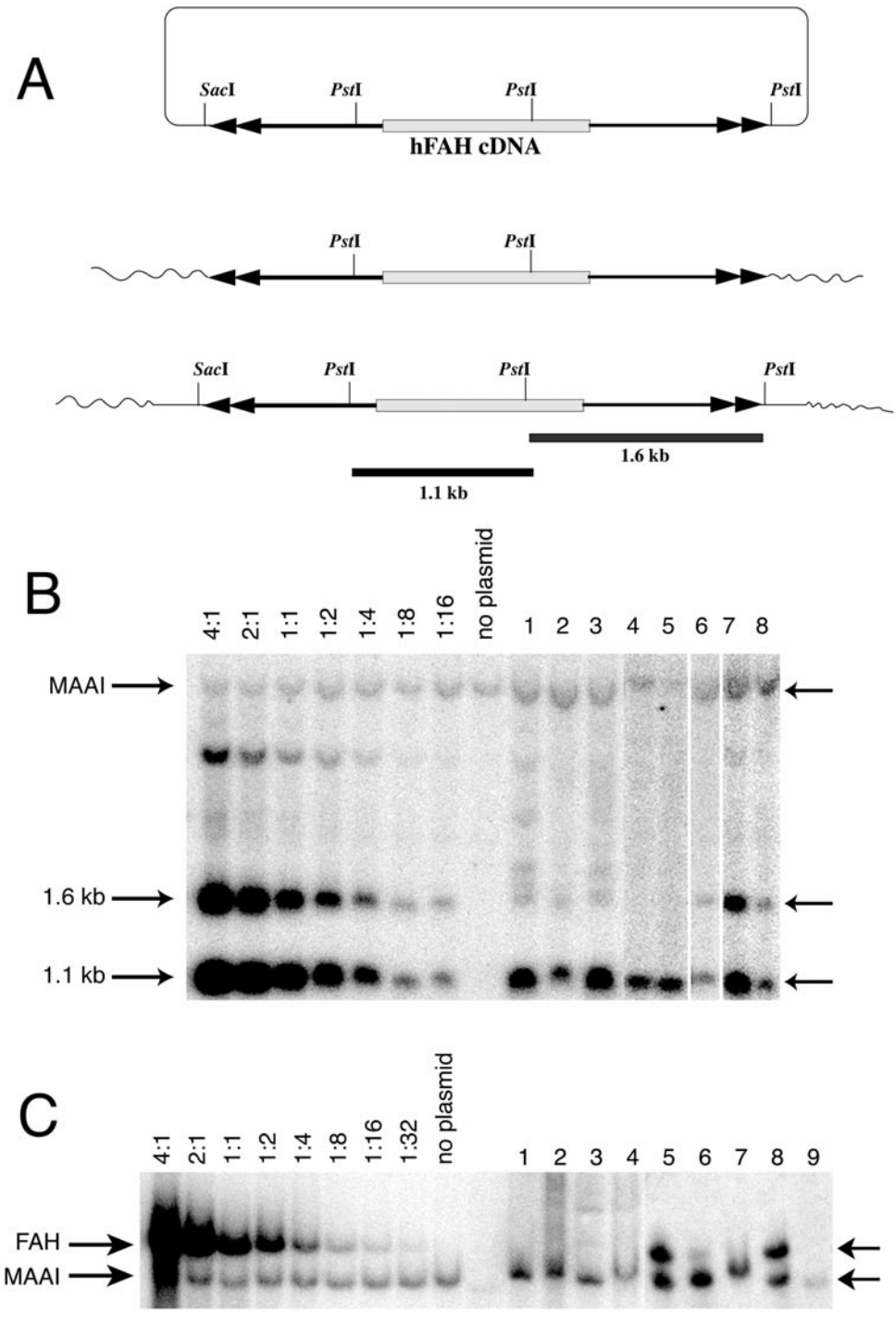

FIG. 3. Southern blotting to determine transposon copy number. (A) Schematic representation of different forms of the FAH transposon. The top shows circular plasmid and the location of the 1.4-kb hFAH cDNA probe. The middle depicts the structure of transposase-mediated integration. Plasmid DNA is drawn with straight lines, genomic DNA with a wavy line. The *Pst*I site adjacent to the inverted repeat is lost, resulting in the absence of a detectable 1.6-kb band. At the bottom a random integration event is shown. The *Pst*I site is preserved, resulting in the appearance of a 1.6-kb junction fragment. (B) Southern blot of liver genomic DNA digested with *Pst*I and simultaneously hybridized with both an *FAH* and an *MAAI* probe. The standard samples are seen on the left side of the blot with transposon copy numbers of 4, 2, 1, etc., copies/diploid genome equivalent. The top band is the MAAI genomic fragment against which the FAH signals were normalized. The 1.1- and 1.6-kb FAH bands derived from the transposon are indicated. Lanes 1–5 and 7, FAH transposon + wild-type SB: samples from secondary serial transplantation recipients (lanes 1–3), 90 days of selection (lanes 4 and 5), and 25 days of selection (lane 7). Lanes 6 and 8, FAH transposon + mutant SB: 90 days of selection (lane 6) and 25 days of selection (lane 8). The 1.6-kb band indicative of episomal or randomly integrated transposon can be prominently seen in lanes 6–8. However, a faint 1.6-kb band is also present in the wild-type SB-treated samples, indicating a low (<2%) frequency of random integration. (C) Southern blot of liver genomic DNA digested with *Sac*I and simultaneously hybridized with both an *FAH* and an *MAAI* probe. The presence of unintegrated transposon plasmid results in the presents of a 6.7-kb FAH band, detectable only in samples obtained on day 25 after plasmid injection (lanes 5, 6, and 8). After 90 days of selection or longer, no episomal vectors are detected regardless of whether wild-type (lanes 1, 3, 4, 7, and 9) or mutated (2) SB was used.

DISCUSSION

Most of the work aimed at treating genetic diseases, including inborn errors of metabolism affecting the liver, by gene therapy has focused on the use of viral vectors such retroviral, adenoviral, and adeno-associated virus vectors [41]. Nonviral gene transfer methods have received less attention because it was thought that naked DNA constructs lacked the ability to result in stable chromosomal integration and persistent gene expression. Recently, however, several systems have been developed that allow

doi:10.1006/mthe.2002.0812

TABLE 5: Estimation of transposon copy number

	pT-hFAH + pCMV-SB $n = 8$	pT-hFAH + pCMV-mSB $n = 3$	Serially transplanted $n = 5$
Total copy number	0.47 ± 0.25	0.38 ± 0.3	0.42 ± 0.04
	(0.1–0.8)	(0.04–0.6)	(0.4–0.5)
Corrected copy number	0.78	0.63	0.7
Random integration	0.006 ± 0.009	0.19 ± 0.27	ND
	(0–0.02)	(0.02–0.5)	
Episomal plasmid	0	0	0

Genomic DNA from long-term survivors (5 months off NTBC) treated with different plasmid combinations and from serially transplanted mice was analyzed. The total transposon copy number (1.1-kb *Pst*I band), random integration copy number (1.6-kb *Pst*I band), and levels of episomal plasmid (6.7-kb *Sac*I band) are indicated as the averages ± standard deviation. The corrected copy number considers the fact that only 60% of liver DNA is from hepatocytes. The minimum and maximum values for each group are given in brackets. ND, not determined.

stable integration of plasmid constructs into chromosomal DNA by either transposition [2] or recombination [42]. The Tc1-like transposon *Sleeping Beauty* has shown particular promise and has already been applied for *in vivo* gene therapy in mouse liver [18]. In this original study, high levels of stable factor IX expression were achieved and it was estimated that the absolute frequency of stable integration approached 2% with a single hydrodynamic injection of both transposon and transposase plasmids. Despite this relatively high efficiency, the stably transfected cells represented only a small portion of the total liver and thus molecular studies regarding the nature of the integration events were limited. In this report, we have further studied the potential utility of this transposon system *in vivo* using the FAH knockout mouse model. This model was chosen because it permits selection of stably transfected hepatocytes, thus facilitating analyses of transposon-corrected cells by Southern blot and histological methods.

The absolute frequency of transposase-mediated FAH gene transfer observed here was surprisingly low at only $2.6 \pm 3.1 \times 10^{-4}$ (1/3800). However, this observation is most likely explained by the low initial transfection efficiencies achieved by hydrodynamic injection in FAH mutant mice. We have found that the frequencies are typically less than 1%, i.e., 10- to 20-fold lower than reported by the literature [40] and found by us in other strains of mice. The precise reason for this atypical behavior is currently unknown, but it is likely that the transient hepatic injury induced by hydrodynamic transfection is more severe in FAH knockout mice. When the integration efficiency was corrected for transfection efficiency, we found that ~4% of transfected hepatocytes had undergone a transposase-mediated integration event and expressed

TABLE 6: Junction fragments rescued by inverse PCR

Clone	Junction	Homology
1	CAACTG**TA**tgtttatgagta	BC005708 *Mus musculus,* similar to serine/threonine protein kinase MASK
2	CAACTG**TA**ggttcgaaccat	gi|4884663| *Mus musculus* aldehyde oxidase (Aox) gene, exon 26
3	TCCAAC-~~ttaagtgtatgtaaacttccgacttcaactg~~-**ac**tatcatccgt	XM_140589.1 *Mus musculus,* similar to lame duck; myoblasts incompetent; gleeful (LOC226078)
4	CAACTG**TA**catgcttgttac	No homology
5	CAACTG**TA**tactattatatc	21212499 Mouse DNA sequence from clone RP23-380L6 on chromosome 13
6	CAACTG**TA**agcccttagcta	gb|AC083909.20|AC083909 *Mus musculus* BAC RP23-424A2
7	CAACTG**TA**tgccacagacca	No homology
8	CAACTG**TA**ccttgctgtaac	emb|AL627435.18| Mouse DNA sequence from clone RP23-3M14 on chromosome X

The junctions of transposon to genomic DNA are shown. The transposon sequence is in uppercase, the genomic DNA in lowercase. All clones but one (No. 3) displayed the characteristic molecular signature of transposition (TA dinucleotide in bold). Clone 3 had a deletion in the terminal portion of the transposon IR sequence (stroked). Known integration sites are listed.

FAH. If only nodules were counted as stable integration events, the average integration frequency still was lower at 0.5% than that previously reported [18] but still significant. The FAH expression was stable and led to the phenotypic correction of the metabolic liver disease and secondary renal damage. Transposon-modified hepatocytes could be serially transplanted and never formed tumors despite at least 30 cell doublings. Thus, the *Sleeping Beauty* transposon/transposase does not appear to be associated with the induction of genomic instability.

Furthermore, our results indicated that the inclusion of the transposon and transposase on the same plasmid (*cis*-construct) resulted in much lower gene transfer frequencies. This was not unexpected, because it had previously been shown that the optimal ratio of transposase to transposon is ~1:25 when the transposase expression is driven by the CMV promoter [18]. The level of transposase expression in the transfected hepatocytes was likely too high. Therefore, it might be necessary to test additional *cis*-acting constructs utilizing weaker promoters in future *in vivo* experiments to maximize the power of this integrative nonviral system fully.

Southern blot analysis permitted the accurate quantitation of the copy number and the analysis of the integration events. Importantly, the copy number of FAH-expressing transposon per genome was close to 1. This indicates that virtually all transposase-mediated integration events were "productive" and associated with FAH gene expression. This is in contrast to some other gene transfer systems, most notably AAV, which results in multiple copies per hepatocyte [43]. Transposition may therefore occur into regions of the genome that are transcriptionally active and hence accessible. In the case of the wild-type transposase, >95% of all integration events resulted in the loss of restriction sites directly adjacent to the inverted repeats, consistent with the established transposition mechanism. In contrast, many integrations found in mice injected with mutated transposase showed evidence for retention of parts of the plasmid backbone, suggesting random integration events. In addition, the absolute frequency of integration was much lower in animals injected with mutated transposase.

Overall, the results obtained here confirm the therapeutic potential of the *Sleeping Beauty* transposon/transposase system for *in vivo* gene therapy application in the liver. Despite its promise, however, the low absolute gene transfer efficiency seen in our experiments illustrates that the technology must be improved before successful clinical application can be contemplated. There are two major rate-limiting steps. First, DNA uptake by hepatocytes *in vivo* is not very efficient, even with the hydrodynamic method of injection. Although hydrodynamic injection works reasonably well in rodents, it is a much too traumatic procedure to be considered for use in humans. Safer methods of delivery including liposomes and polyethyleneimine-complexed DNA may solve the problem in the future [44,45]. Another approach is to incorporate the *Sleeping Beauty* system into a viral vector with hepatotropism. In fact, such a vector was recently tested successfully *in vivo* [46].

The second rate-limiting step is the actual integration once the DNA has entered the cell. Once a hepatocyte has taken up the naked DNA, transposition is relatively efficient (1–5%), even with the currently used two-plasmid system. Nonetheless, improved constructs that contain the transposable element and the transposase *in cis* in the same plasmid and express optimal levels of transposase may further enhance this efficiency. It is also possible that the *Sleeping Beauty* transposase enzyme could be improved to catalyze integration more efficiently, perhaps by *in vitro* evolution [47].

The use of naked DNA for the treatment of genetic liver diseases has several obvious potential advantages over more conventional gene transfer vectors. These include the ability to generate the required plasmids in large quantities at reasonable cost and the low immunogenicity of naked DNA, which should allow multiple rounds of readministration. The main rate-limiting step for future *in vivo* use of this method appears to be the uptake of DNA into hepatocytes. We are hopeful that the now clearly documented potential for stable gene transfer with plasmid DNA with energize the search for safe methods to achieve this goal.

MATERIALS AND METHODS

Vector construction. The plasmids pCMV-SB (expressing the SB transposase under the control of the CMV promoter) and pCMV-mSB (encoding a mutated, nonfunctional transposase) have been reported previously [18]. The full-length human FAH cDNA contained in phFAFFA2 (1.4 kb) [27] was cloned into a blunted *Eco*RI site of the expression plasmid pCD-SRα [28]. The resulting plasmid pCD-SRαhFAH expresses the FAH enzyme under the transcriptional control of the SRα promoter and contains an SV40 polyadenylation sequence (entire expression cassette 3.46 kb). This cassette was released by digestion with *Sal*I and cloned into pT-MCS [18] at the *Xho*I site between the IR sequences. The resulting 7-kb plasmid pT-hFAH contained a 4.38-kb transposon.

A synthetic oligonucleotide linker containing the restriction sites *Xho*I–*Nar*I–*Xho*I was cloned into the *Sal*I restriction site adjacent to the 3′ IR sequence. In the resulting plasmid, the hFAH transposon was now contained within a 5-kb *Nar*I fragment, which was cloned into the *Nar*I restriction site of the plasmid pCMV-SB. The resulting construct, pT-hFAH-SBcis, contains both the hFAH transposon and the CMV-promoter-driven transposase expression cassette *in cis*.

Animal husbandry, transposon injection, and hepatocyte selection. Six- to eight-week-old mice of the $FAH^{\Delta exon5}$ strain [19] were treated according to the NIH *Guidelines for Animal Care* and with approval of the institutional animal care and utilization committee of the Oregon Health and Sciences University. Plasmid DNA diluted in 0.9% NaCl (2 ml) was hydrodynamically injected into the tail vein over 5–8 s as previously described [29,30]. All $FAH^{\Delta exon5}$ breeders and mutant animals were treated with NTBC containing water at a concentration of 7.5 mg/L (provided by S. Lindstedt, Gothenborg, Sweden) for a week after injection [31]. To allow the expansion of the FAH-expressing hepatocytes, animals were then taken off the protective drug and the body weight was measured weekly. NTBC therapy was reinstated for 1 week whenever animals lost more than of 25% their

doi:10.1006/mthe.2002.0812

pretreatment weight. After weight restoration, NTBC was again discontinued.

Hepatocyte transplantation. Transposon-injected FAH$^{-/-}$ mice that survived for more than 3 months off NTBC were used as hepatocyte donors for serial transplantation experiments as previously described [32]. During the first round of serial transplantation 500,000 hepatocytes were injected into the spleen of isogenic FAH$^{-/-}$ mice. For all subsequent rounds of transplantation we used either 10,000 or 500,000 hepatocytes.

Liver function tests. Animals were sacrificed by decapitation and blood was collected in Microtainer plasma separator tubes with lithium heparin (Becton–Dickinson Vacutainer Systems, Franklin Lakes, NJ). After brief centrifugation the plasma was frozen at −80°C. Twenty microliters of plasma was mixed with 80 μl of a 7% (w/v) bovine serum albumin solution and assayed for aspartate serine aminotransferase, bilirubin, and creatinine levels using a Kodak Ektachem 700 chemistry analyzer (Eastman Kodak, Rochester, NY).

Histology and immunohistology. Liver tissues fixed in 10% phosphate-buffered formalin, pH 7.4, were dehydrated in 100% ethanol and embedded in paraffin wax at 58°C. Four-micrometer sections were rehydrated and stained with hematoxylin and eosin and with a polyclonal rabbit antibody against rat FAH (kindly provided by Robert Tanguay, University of Laval, Quebec, Canada). The antibody was diluted in PBS, pH 7.4, and applied at concentrations of 1:300,000 at 37°C for 30 min. Endogenous peroxidase activity was blocked with 3% H_2O_2 and methanol. Avidin and biotin pretreatment was used to prevent endogenous staining. The secondary antibody was biotinylated goat anti-rabbit IgG used at 1:250 dilution (BA-1000; Vector Laboratories, Burlingame, CA). Color development was performed with the AEC detection kit (Cat. No. 250-020; Ventana Medical Systems, Tucson, AZ).

Determination of the integration efficiency. FAH$^{-/-}$ mice were injected via the tail vein with different combinations of plasmids (described under Results). After 25 days of *in vivo* selection (i.e., no NTBC), the liver was harvested and sections of at least 0.7 cm^2 were analyzed by FAH immunohistology for the presence of FAH$^+$ hepatocytes using a Leica microscope DM RX (Leica Microsystems, Bannockburn, IL). FAH$^+$ clusters (two or more cells) and FAH$^+$ single hepatocytes present in a given histological section were counted and noted separately. The precise surface area of each section was measured by scanning the glass slides along with a size standard using a Microtec 2 scanner at a resolution of 300 dpi. Adobe PhotoShop 5.02 software was then used to select and count the pixels corresponding to the liver sections. FAH mutant liver contains 186,000 hepatocytes/cm^2 [33]. Since clonal hepatocyte nodules are larger than single hepatocytes, they will be more readily detected in a two-dimensional section. The correction factor required to adjust calculations of nodule frequency was calculated as previously described [33].

We performed the following calculations to produce the numbers shown in Tables 1–3. The initial transfection frequency (Table 1) was determined by counting the number of FAH$^+$ hepatocytes on day 3 after injection and dividing this number by the total number of hepatocytes scored. The absolute frequencies of FAH$^+$ single cells and clusters (Table 2) represent the raw, uncorrected number of events divided by the total number of hepatocytes in the section. The mean, median, and standard deviation given in the table were calculated using Prism 3 software (GraphPad). The corrected integration frequencies (Table 3) represent data from Table 2 that have been adjusted in two ways. First, the absolute numbers were corrected for the estimated initial transfection frequency. Calculations were made for the observed average transfection frequency (0.5%) as well as the highest observed frequency (10%). In addition, the nodule frequencies in Table 3 were corrected for nodule size. The larger the nodules, the lower the estimated frequency [33].

Southern blot analysis. For Southern blots, liver DNA was isolated from liver freshly obtained or from liver frozen at −80°C. At least 350 mg of tissue (~1/3 of entire liver mass) was used for DNA isolation. Capillary transfer and hybridizations were performed according to standard protocols [34].

For quantification of the transposon copy number, liver DNA was digested with *Pst*I or *Sac*I (Roche, Indianapolis, IN) and probed with a 1.4-kb *Eco*RI fragment isolated from phFAFFA2 containing the entire coding sequence of the human FAH cDNA. As an internal control, we used a 200-bp fragment from a genomic region of the mouse maleylacetoacetate isomerase (MAAI) gene [35]. The intensity of the FAH bands was normalized to the relative intensity of the corresponding MAAI control band and quantified by Phosphoimager analysis. Calculations for copy number determination were performed as described previously [36].

Inverse PCR. All PCRs were performed as described in standard protocols [34]. Mouse liver genomic DNA (2 μg) from repopulated mice was digested with *Sau*3AI (Fermentas, Hanover, MD) and diluted to 100 μl and then different amounts of digested DNA (1 μg, 100 ng, or 10 ng) were circularized with a standard ligation reaction at a final volume of 100 μl. Self-ligated template DNA was then used for the first round of PCR amplification with oligonucleotide pairs designed for the left end of the transposon sequences (MG1094, AAACGAGTTTTAATGACTCCAAC, and MG1118, AGGCAGGCAGAAGTATGC). The cycling conditions were 94°C for 45 s, 60°C for 45 s, 72°C for 4 min repeated for 30 cycles and followed by 72°C for 10 min. A second round of amplification was performed using a nested pair of oligonucleotide primers: MG1096, 5′-AAAGATCGAGTTTTAATGACTCCAACTTAA, and MG1119, 5′-AGGCAGAAGTATGCAAAGC. PCR products were separated on a 3% agarose gel and the PCR specificity was determined by Southern blot hybridization using another nested oligonucleotide (MG1100, 5′-TGTAAACTTCCGACTTCAACT). All reactions displayed positive signals (data not shown).

Inverse PCR products were cloned into the pCRII vector (Invitrogen, Carlsbad, CA), sequenced, and analyzed by BLASTn homology database searches. The significance score for the indicated homologies was 1×10^{-20}.

ACKNOWLEDGMENTS

We thank Hiroyuki Nakai (Stanford, CA) for helpful discussions, Jose-Manuel Fernandez-Canon (Portland, OR) for the MAAI mouse genomic probe, Robert Tanguay (Québec City, Canada) for the anti-FAH antibody, and Angela Major (Houston, TX) for technical assistance. This work was supported by NIH Grants RO1-DK48252 to M.G. and RO1-DK49022 to M.A.K. and NRSA Grant 5F32DK10084 to E.M.

RECEIVED FOR PUBLICATION SEPTEMBER 3, 2002; ACCEPTED OCTOBER 28, 2002.

REFERENCES

1. Hamer, L., DeZwaan, T. M., Montenegro-Chamorro, M. V., Frank, S. A., and Hamer, J. E. (2001). Recent advances in large-scale transposon mutagenesis. *Curr. Opin. Chem. Biol.* **5:** 67–73.
2. Ivics, Z., Hackett, P. B., Plasterk, R. H., and Izsvak, Z. (1997). Molecular reconstruction of Sleeping Beauty, a Tc1-like transposon from fish, and its transposition in human cells. *Cell* **91:** 501–510.
3. Fischer, S. E., Wienholds, E., and Plasterk, R. H. (2001). Regulated transposition of a fish transposon in the mouse germ line. *Proc. Natl. Acad. Sci. USA* **98:** 6759–6764.
4. Plasterk, R. H. (1996). The Tc1/mariner transposon family. *Curr. Top. Microbiol. Immunol.* **204:** 125–143.
5. Vos, J. C., and Plasterk, R. H. (1994). Tc1 transposase of Caenorhabditis elegans is an endonuclease with a bipartite DNA binding domain. *EMBO J.* **13:** 6125–6132.
6. Lampe, D. J., Churchill, M. E., and Robertson, H. M. (1996). A purified mariner transposase is sufficient to mediate transposition in vitro. *EMBO J.* **15:** 5470–5479.
7. Lampe, D. J., Akerley, B. J., Rubin, E. J., Mekalanos, J. J., and Robertson, H. M. (1999). Hyperactive transposase mutants of the Himar1 mariner transposon. *Proc. Natl. Acad. Sci. USA* **96:** 11428–11433.
8. Catteruccia, F., *et al.* (2000). Stable germline transformation of the malaria mosquito Anopheles stephensi. *Nature* **405:** 959–962.
9. Raz, E., van Luenen, H. G., Schaerringer, B., Plasterk, R. H., and Driever, W. (1998). Transposition of the nematode Caenorhabditis elegans Tc3 element in the zebrafish Danio rerio. *Curr. Biol.* **8:** 82–88.
10. Fadool, J. M., Hartl, D. L., and Dowling, J. E. (1998). Transposition of the mariner element from Drosophila mauritiana in zebrafish. *Proc. Natl. Acad. Sci. USA* **95:** 5182–5186.
11. Sherman, A., *et al.* (1998). Transposition of the Drosophila element mariner into the chicken germ line. *Nat. Biotechnol.* **16:** 1050–1053.

12. Schouten, G. J., van Luenen, H. G., Verra, N. C., Valerio, D., and Plasterk, R. H. (1998). Transposon Tc1 of the nematode Caenorhabditis elegans jumps in human cells. *Nucleic Acids Res.* **26:** 3013–3017.

13. Klinakis, A. G., Zagoraiou, L., Vassilatis, D. K., and Savakis, C. (2000). Genome-wide insertional mutagenesis in human cells by the Drosophila mobile element Minos. *EMBO Rep.* **1:** 416–421.

14. Luo, G., Ivics, Z., Izsvak, Z., and Bradley, A. (1998). Chromosomal transposition of a Tc1/mariner-like element in mouse embryonic stem cells. *Proc. Natl. Acad. Sci. USA* **95:** 10769–10773.

15. Dupuy, A. J., *et al.* (2002). Mammalian germ-line transgenesis by transposition. *Proc. Natl. Acad. Sci. USA* **99:** 4495–4499.

16. Horie, K., *et al.* (2001). Efficient chromosomal transposition of a Tc1/mariner- like transposon Sleeping Beauty in mice. *Proc. Natl. Acad. Sci. USA* **98:** 9191–9196.

17. Wolff, J. A. (1997). Naked DNA transport and expression in mammalian cells. *Neuromuscul. Disord.* **7:** 314–318.

18. Yant, S. R., *et al.* (2000). Somatic integration and long-term transgene expression in normal and haemophilic mice using a DNA transposon system. *Nat. Genet.* **25:** 35–41.

19. Grompe, M., *et al.* (1993). Loss of fumarylacetoacetate hydrolase is responsible for the neonatal hepatic dysfunction phenotype of lethal albino mice. *Genes Dev.* **7:** 2298–2307.

20. Overturf, K., *et al.* (1998). Ex vivo hepatic gene therapy of a mouse model of hereditary tyrosinemia type I. *Hum. Gene Ther.* **9:** 295–304.

21. Manning, K., Al-Dhalimy, M., Finegold, M., and Grompe, M. (1999). In vivo suppressor mutations correct a murine model of hereditary tyrosinemia type I. *Proc. Natl. Acad. Sci. USA* **96:** 11928–11933.

22. Overturf, K., *et al.* (1996). Hepatocytes corrected by gene therapy are selected in vivo in a murine model of hereditary tyrosinaemia type I. *Nat. Genet.* **12:** 266–273.

23. Lagasse, E., *et al.* (2000). Purified hematopoietic stem cells can differentiate into hepatocytes in vivo. *Nat. Med.* **6:** 1229–1234.

24. Overturf, K., *et al.* (1997). Adenovirus-mediated gene therapy in a mouse model of hereditary tyrosinemia type I. *Hum. Gene Ther.* **8:** 513–521.

25. Chen, S. J., Tazelaar, J., Moscioni, A. D., and Wilson, J. M. (2000). In vivo selection of hepatocytes transduced with adeno-associated viral vectors. *Mol. Ther.* **1:** 414–422.

26. Nakai, H., *et al.* (2002). Helper-independent and AAV-ITR-independent chromosomal integration of double-stranded linear DNA vectors in mice. *Mol. Ther.* (in press).

27. Phaneuf, D., *et al.* (1991). Cloning and expression of the cDNA encoding human fumarylacetoacetate hydrolase, the enzyme deficient in hereditary tyrosinemia: Assignment of the gene to chromosome 15. *Am. J. Hum. Genet.* **48:** 525–535.

28. Takebe Y., *et al.* (1988). SR alpha promoter: An efficient and versatile mammalian cDNA expression system composed of the simian virus 40 early promoter and the R-U5 segment of human T-cell leukemia virus type 1 long terminal repeat. *Mol. Cell. Biol.* **8:** 466–472.

29. Song, Y. K., Liu, F., Zhang, G., and Liu, D. (2002). Hydrodynamics-based transfection: Simple and efficient method for introducing and expressing transgenes in animals by intravenous injection of DNA. *Methods Enzymol.* **346:** 92–105.

30. Liu, F., Song, Y., and Liu, D. (1999). Hydrodynamics-based transfection in animals by systemic administration of plasmid DNA. *Gene Ther.* **6:** 1258–1266.

31. Grompe, M., *et al.* (1995). Pharmacological correction of neonatal lethal hepatic dysfunction in a murine model of hereditary tyrosinaemia type I. *Nat. Genet.* **10:** 453–460.

32. Overturf, K., al-Dhalimy, M., Ou, C. N., Finegold, M., and Grompe, M. (1997). Serial transplantation reveals the stem-cell-like regenerative potential of adult mouse hepatocytes. *Am. J. Pathol.* **151:** 1273–1280.

33. Wang, X., *et al.* (2002). Kinetics of liver repopulation after bone marrow transplantation. *Am. J. Pathol.* **161:** 565–574.

34. Sambrook, J. R. D. W. e. (2001). *Molecular Cloning: A Laboratory Manual,* 3rd ed. Cold Spring Harbor Laboratory Press, Cold Spring Harbor, NY.

35. Fernandez-Canon, J. M., Hejna, J., Reifsteck, C., Olson, S., and Grompe, M. (1999). Gene structure, chromosomal location, and expression pattern of maleylacetoacetate isomerase. *Genomics* **58:** 263–269.

36. Noll, M., Bateman, R. L., D'Andrea, A. D., and Grompe, M. (2001). Preclinical protocol for in vivo selection of hematopoietic stem cells corrected by gene therapy in Fanconi anemia group C. *Mol. Ther.* **3:** 14–23.

37. Gusella, G. L., *et al.* (2002). Lentiviral gene transduction of kidney. *Hum. Gene Ther.* **13:** 407–414.

38. Mujtaba, T., Han, S. S., Fischer, I., Sandgren, E. P., and Rao, M. S. (2002). Stable expression of the alkaline phosphatase marker gene by neural cells in culture and after transplantation into the CNS using cells derived from a transgenic rat. *Exp. Neurol.* **174:** 48–57.

39. Chen, Z. Y., *et al.* (2001). Linear DNAs concatemerize in vivo and result in sustained transgene expression in mouse liver. *Mol. Ther.* **3:** 403–410.

40. Zhang, G., Budker, V., and Wolff, J. A. (1999). High levels of foreign gene expression in hepatocytes after tail vein injections of naked plasmid DNA. *Hum. Gene Ther.* **10:** 1735–1737.

41. Kay, M. A., Glorioso, J. C., and Naldini, L. (2001). Viral vectors for gene therapy: The art of turning infectious agents into vehicles of therapeutics. *Nat. Med.* **7:** 33–40.

42. Thyagarajan, B., Olivares, E. C., Hollis, R. P., Ginsburg, D. S., and Calos, M. P. (2001). Site-specific genomic integration in mammalian cells mediated by phage phiC31 integrase. *Mol. Cell. Biol.* **21:** 3926–3934.

43. Nakai, H., *et al.* (2001). Extrachromosomal recombinant adeno-associated virus vector genomes are primarily responsible for stable liver transduction in vivo. *J. Virol.* **75:** 6969–6976.

44. Kren, B. T., Bandyopadhyay, P., and Steer, C. J. (1998). In vivo site-directed mutagenesis of the factor IX gene by chimeric RNA/DNA oligonucleotides. *Nat. Med.* **4:** 285–290.

45. Bandyopadhyay, P., Ma, X., Linehan-Stieers, C., Kren, B. T., and Steer, C. J. (1999). Nucleotide exchange in genomic DNA of rat hepatocytes using RNA/DNA oligonucleotides. Targeted delivery of liposomes and polyethyleneimine to the asialoglycoprotein receptor. *J. Biol. Chem.* **274:** 10163–10172.

46. Yant, S. R., *et al.* (2002). Transposition from a gutless adeno-transposon vector stabilizes transgene expression in vivo. *Nat. Biotechnol.* **20:** 999–1005.

47. Stemmer, W. P. (1994). Rapid evolution of a protein in vitro by DNA shuffling. *Nature* **370:** 389–391.